Multimode Synchronization and Communication Using Unidirectionally Coupled Semiconductor Lasers

Javier Martín Buldú, Jordi García-Ojalvo, and M. C. Torrent

***Abstract*—We study numerically the synchronization of two multimode semiconductor lasers unidirectionally coupled in an open-loop configuration, focusing on the comparison with the results obtained in the single-mode case. Anticipative and isochronous synchronization, and their range of validity, are analyzed from the point of view of the total lasing output, and the synchronization between individual modes is studied. Selective injection is also examined and compared with global injection. In light of these results, message encoding and decoding via multimode synchronization is analyzed.**

***Index Terms*—Anticipated synchronization, chaos synchronization, chaotic communications, multimode lasers, semiconductor lasers.**

I. Introduction

THE application of chaotic lasers to private communications has been a field of special interest in recent years [1], [2]. In particular, encoding a message in the output intensity of a chaotic semiconductor laser has been proved, both numerically [3]–[6] and experimentally [7]–[9], to be an efficient way of transmitting information. Among the different methods that lead a semiconductor laser to have a chaotic output, feedback (both optoelectronic [7], [9] and purely optical [8]) is widely used for communication purposes. Most of the chaotic communication schemes available, including chaos modulation [10], [11] and chaos shift keying [12], are based on the synchronization between the receiver laser and the chaotic transmitter output [13], [14]. This requirement limits the range of operation of chaotic communication systems and demands a good understanding of the synchronization of chaotic lasers. Recent numerical studies have focused on the types of synchronization and their range of validity in the case of single-mode semiconductor lasers with optical feedback [15]. Experimental results qualitatively reproduce the numerical observations, although most experimental studies use mainly multimode (Fabry–Perot) semiconductor lasers. However, synchronization [16] and data transmission [17], [18] in multimode semiconductor lasers have not been as deeply and systematically studied as the single-mode case. Different models have been used to describe the dynamics of multimode semiconductor lasers. Viktorov and Mandel [19] developed a model based on the Tang *et al.* description [20], where two sets of rate equations describing the evolution of the electrical field and carrier number of each longitudinal mode were considered. Rogister *et al.* [21] introduced a model based on an extension of the Lang–Kobayashi model [22], with a rate equation for each longitudinal mode and a single equation for describing the total carrier number. More accurate models have been recently developed with the aim of considering the role of spatial carrier dynamics and spatial hole burning [23], [24].

In the present paper, we perform a systematic numerical study of different types of synchronization in coupled multimode semiconductor lasers and compare the results with the ones obtained for the single-mode case. We use a model based on [21] due to its simplicity when compared with other multimode models and to the fact that this model has successfully described the dynamics of a multimode semiconductor laser with optical feedback [25]. The validity of the assumptions of this model (in relation to both its Lang–Kobayashi character and its treatment of modal dynamics) should be checked in further work employing more precise multimode models.

Although the results are centered in the behavior of the total intensity, modal intensities and their temporal dynamics are also analyzed, and the synchronization between corresponding modes of the transmitter and receiver is examined. Selective injection (where only one mode of the emitter is injected into the receiver) is also studied, in order to compare its efficiency with global (all-to-all) injection. Finally, message transmission using multimode synchronization is examined.

II. The Model

We consider the communication system depicted in Fig. 1. A multimode diode laser LD-t is subject to optical feedback from an external mirror M, which affects all longitudinal modes equally (the modes are symbolically represented by parallel horizontal lines in the figure). The (chaotic) output of this laser is injected into a second laser LD-r, which is not subject to feedback itself (this is sometimes known as an open-loop communication scheme). An optical isolator OI ensures that light propagates exclusively from the transmitter LD-t to the receiver LD-r. Furthermore, in parts of the following we consider that a frequency-selective filter allows only injection of one longitudinal

Manuscript received November 6, 2003; revised January 29, 2004. This work was supported by the EC project IST-2000-29683 OCCULT, by MCyT-FEDER Spain (projects BFM2002-04369 and BFM2003-07850), and by the Generalitat de Catalunya (project 2001SGR00223).

J. M. Buldú and M. C. Torrent are with the Departament de Física i Enginyeria Nuclear, Universitat Politècnica de Catalunya, E-08222 Terrassa, Spain (e-mail: javier.martin-buldu@upc.es; carme.torrent@upc.es).

J. García-Ojalvo is with the Center for Applied Mathematics, Cornell University, Ithaca, NY 14853 USA, on leave from the Departament de Física i Enginyeria Nuclear, Universitat Politècnica de Catalunya, E-08222 Terrassa, Spain (e-mail address: jordi.g.ojalvo@upc.es).

Digital Object Identifier 10.1109/JQE.2004.828230

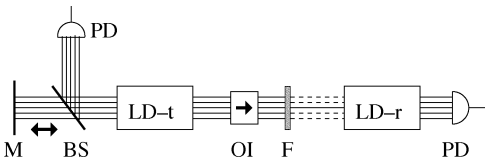

Fig. 1. Schematic setup of the communication system considered. The different longitudinal modes of the transmitter laser diode LD-t are schematically represented by horizontal lines. The transmitter laser is subject to optical feedback from the external mirror M. An optical isolator OI ensures unidirectional propagation from the transmitter to the receiver laser LD-r. A filter F may be used to allow selective injection of only one longitudinal mode into the receiver. The dynamical behavior of both lasers can be measured by the photodiodes PD. In the transmitter laser, a beam splitter BS may be used to direct part of the laser output to the photodetector.

mode of the transmitter into the receiver (what we call selective injection), as compared to the situation where no such filter is present, and all modes of the transmitter are injected into the receiver (what we call global injection).

We use a multimode model to describe the evolution of the slow-varying complex envelope $E_m^{(t,r)}(t)$ of the mth longitudinal mode of the electric field generated by the transmitter/receiver (denoted by the superindices t/r, respectively) and the corresponding carrier number $N^{(t,r)}(t)$, assuming that the carriers are shared by all modes in each laser [21]. The model is considered an extension (see for instance [16]) of the Lang–Kobayashi equations describing the dynamical behavior of semiconductor lasers with optical feedback [22]:

$$\frac{dE_m^{(t)}}{dt} = \frac{1}{2}(1+i\alpha)\left[G_m\left(N^{(t)}\right)-\gamma\right]E_m^{(t)}(t) + \kappa_t E_m^{(t)}(t-\tau_t)e^{-i\omega_{0m}\tau_t} + \sqrt{2\beta N^{(t)}}\zeta_m^{(t)}(t) \quad (1)$$

$$\frac{dE_m^{(r)}}{dt} = \frac{1}{2}(1+i\alpha)\left[G_m\left(N^{(r)}\right)-\gamma\right]E_m^{(r)}(t) + \kappa_{c,m} E_m^{(t)}(t-\tau_c)e^{i\omega_{0m}\tau_c} + \sqrt{2\beta N^{(r)}}\zeta_m^{(r)}(t) \quad (2)$$

$$\frac{dN^{(t,r)}}{dt} = \gamma_e\left[CN_{\rm th} - N^{(t,r)}(t)\right] - \sum_{m=1}^{M} G_m\left(N^{(t,r)}\right)\left|E_m^{(t,r)}\right|^2. \quad (3)$$

The transmitter field equation (1) is subject to its own delayed feedback, while the delayed term in the receiver field equation (2) corresponds to the injection from the transmitter. We assume zero detuning between the two lasers in order to simplify the model, since this is the situation usually considered experimentally in synchronization and communication applications. The total number of modes in each laser is represented by M. The electric field amplitudes $E_m(t)$ are normalized so that $P_m(t) = |E_m(t)|^2$ measures the photon number in the mth mode. The intrinsic laser parameters are the linewidth enhancement factor α, the cavity loss coefficient γ, and the inverse lifetime of the electron-hole pairs γ_e, all of which are considered to be equal for all modes and for the two lasers. Spontaneous emission is represented by the Langevin noise forces $\zeta_m^{(t,r)}(t)$, which are assumed to be Gaussian and white with zero mean and unity intensity. Carrier noise is not considered at the present level of description; this approximation is common in both single-mode [26] and multimode [6] semiconductor laser models. In the equation for carrier density, C is the normalized injection current and $N_{\rm th}$ is the carrier number at the solitary-laser threshold (given by $C_{\rm th} = 1$, which for the parameters of Table I correspond to a threshold injection current $I_{\rm th}$ =19.8 mA).

TABLE I
PARAMETERS USED IN THE SIMULATIONS

Description	Symbol	Value
Total number of modes	M	5
Linewidth enhancement factor	α	4.0
Cavity loss coefficient	γ	0.238 ps^{-1}
Carrier inverse lifetime	γ_e	6.21×10^{-4} ps^{-1}
Injection current	C	1.015
Internal round-trip time	τ_L	8.5 ps
Gain peak frequency	ω_c	$\omega_c\tau = 0 \bmod 2\pi$
Material gain width	$\Delta\omega_g$	$2\pi\times21.17$ THz
Saturation coefficient	s	1.0×10^{-7}
Differential gain coefficient	g_c	3.2×10^{-9} ps^{-1}
Transparency inversion	N_0	1.25×10^{8}
Feedback strength	κ_t	0.02 ps^{-1}
Feedback time	τ_t	4.0 ns
Coupling strength	κ_c	variable
Coupling time	τ_c	0.0 ns
Spontaneous emission rate	β	5×10^{-10} ps^{-1}*

* except in Figs. 2–5 where $\beta = 0.0$ ps^{-1}

The feedback parameters of the transmitter, namely the feedback level κ_t and the round-trip time of the external cavity τ_t, are assumed to be equal for all modes. The phase shift $\omega_{0m}\tau_t$ appearing in the feedback term is due to the external-cavity round trip, with ω_{0m} representing the nominal frequency of the mth mode, i.e. $\omega_{0m} = \omega_c \pm (m_c - m)\Delta\omega_L$, where ω_c is the frequency of the gain peak of the solitary laser (corresponding to the mode m_c) and $\Delta\omega_L$ is the longitudinal mode spacing given by $\Delta\omega_L = 2\pi/\tau_L$, where τ_L is the internal round-trip time. The value of τ_c has no influence in the quality of synchronization, provided signal degradation during propagation is not large enough to deteriorate the synchronization, as has been reported in single-mode lasers [3]. Hence, for the sake of simplicity, the coupling between the lasers is considered instantaneous (i.e., $\tau_c = 0$). On the other hand, two types of coupling strengths are considered in this paper, according to what is shown in Fig. 1: for the case of global coupling, $\kappa_{c,m}$ is chosen equal for all modes, whereas for selective coupling $\kappa_{c,m}$ is zero for all but one value of m. The mode-dependent gain coefficient G_m is assumed to have a parabolic profile with its maximum centered at m_c, and its expression is considered equal for both lasers as follows:

$$G_m(N) = \frac{g_c(N-N_0)}{1+s\sum_m |E_m(t)|^2}\left[1-\left(\frac{(m_c-m)\Delta\omega_L}{\Delta\omega_g}\right)^2\right] \quad (4)$$

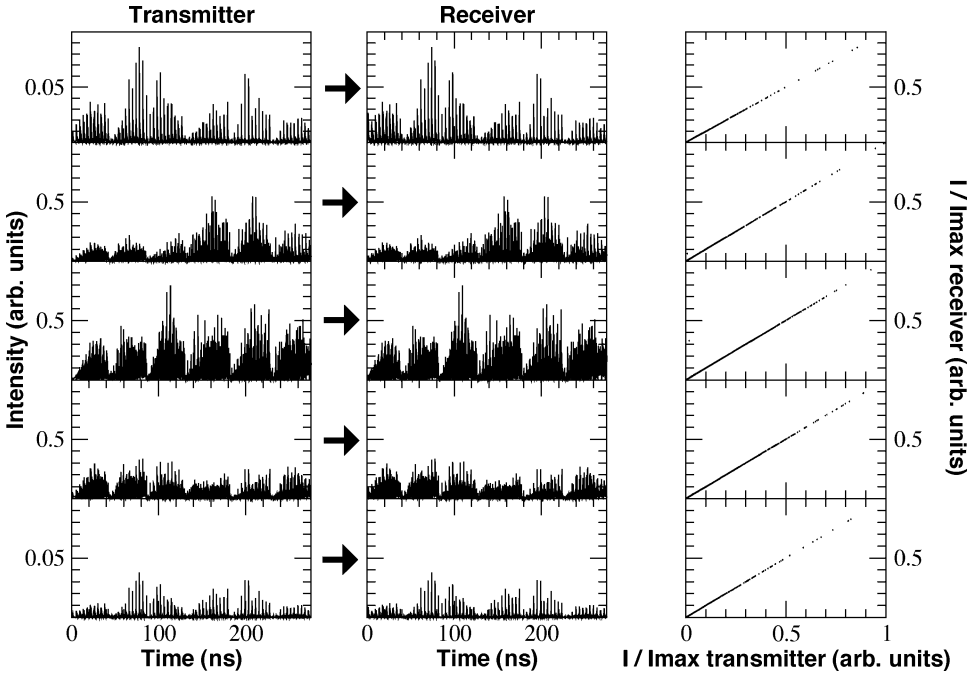

Fig. 2. Transmitter (first column) and receiver (second column) output intensity in the anticipative synchronization regime. It can be observed how all modes (1–5, from top to bottom) synchronize one by one. Although it cannot be appreciated by eye, the output intensity of the receiver is advancing a time τ_t =4 ns the transmitter output. In the third column, we show the corresponding synchronization plots (intensity of receiver versus that of the emitter), where the receiver output has been shifted 4 ns. Spontaneous emission noise is not considered here.

where g_c is the differential gain coefficient at the peak gain of the solitary laser, $\Delta\omega_g$ is the gain width of the laser material, s is the saturation term, and N_0 is the carrier number at transparency. In the calculations presented in the following, we assume five active optical modes (i.e., $M = 5$). The laser parameters used in the simulations are those indicated in Table I.

III. Multimode Synchronization

We have centered our work in the study of two types of synchronization that can be observed in unidirectionally coupled chaotic systems, namely the generalized [27] and the anticipative [28], [29] synchronization. The former type, also called isochronous synchronization, corresponds to the solution $P_r(t) = aP_t(t - \tau_c)$ where the output power of the receiver laser follows the input power of the transmitter with a delay time of τ_c. In the second type, the synchronization corresponds to the identical solution $P_r(t) = P_t(t - \tau_c + \tau_t)$. Note that, in this case, when $\tau_t > \tau_c$, the receiver output can advance in time the transmitter power, hence this synchronization is also called anticipative. In Fig. 2, we present an example of synchronization for the system described in the previous section. The output from the transmitter laser (first column in the figure), which due to the feedback is operating in the low-frequency-fluctuation regime [30], is injected into the receiver laser (whose output is represented in the second column of Fig. 2), which is not subject to feedback itself. The coupling level is set to fulfill the anticipative synchronization condition $\kappa_t = \kappa_c$ (see [29] and [31]), in this particular case $\kappa_t = \kappa_c$ =0.020 ps^{-1}. The third column of Fig. 2 shows the synchronization plot of the two laser intensities when the output intensity of the receiver is shifted the corresponding delay time $\tau_t - \tau_c$ =4 ns (corresponding to the case of anticipative synchronization). As can be observed, the synchronization is achieved in all active modes, due to the fact that each mode is following the anticipative synchronization condition with the corresponding mode of the transmitter (but note the different y-axis scaling of modes 1 and 5 in the left and middle plots of Fig. 2). As a consequence, the total output of both lasers also synchronizes. These results have been obtained without considering spontaneous emission noise, although we have observed that considering it barely modifies the results obtained.

We now focus on the effect that the coupling strength between the lasers has in the quality of synchronization. As a measure of this quality, we compute the cross-correlation function between the output intensities of transmitter and receiver, defined as

$$C(\Delta t) = \frac{\langle (P_t(t) - \langle P_t \rangle)\,(P_r(t + \Delta t) - \langle P_r \rangle) \rangle}{\sqrt{\left\langle (P_t(t) - \langle P_t \rangle)^2 \right\rangle \left\langle (P_r(t) - \langle P_r \rangle)^2 \right\rangle}} \tag{5}$$

where the brackets denote temporal averaging. We can distinguish between the anticipative synchronization ($\Delta t = \tau_c - \tau_t$) and the generalized (isochronous) synchronization $\Delta t = \tau_c$, which is set to 0 in our case. In order to decide which kind of synchronization is observed we analyze the cross-correlation function. As an example of the procedure followed, we show in Fig. 3 two typical cross-correlation functions for the case of anticipating [Fig. 3(a)] and isochronous [Fig. 3(b)] synchronization. The former has been obtained for a configuration fulfilling the anticipating synchronization condition ($\kappa_c = \kappa_t$ =0.02 ps^{-1}), while in the later the coupling strength has been increased (κ_c =0.05 ps^{-1}, with κ_t =0.02 ps^{-1}). If the global maximum of this cross-correlation function is close to 0.9, we consider that both outputs are synchronized, while at the same time the value of Δt corresponding to that maximum

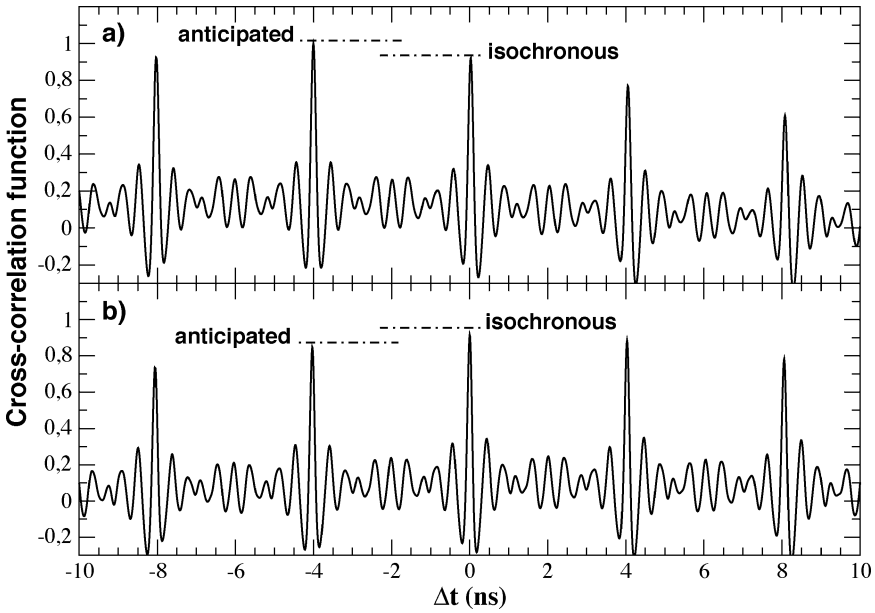

Fig. 3. Cross-correlation function for two different types of synchronization. (a) The global maximum is observed at $\Delta t = -4$ ns, and since its value is higher than 0.9 we consider that we have anticipated synchronization. Note that the correlation also has a local maximum at $\Delta t = 0$ ns which indicates that both outputs have also a good correlation for this Δt. (b) An example of isochronous synchronization, where the cross-correlation function has a global maximum at $\Delta t = 0$ ns, corresponding to the coupling time.

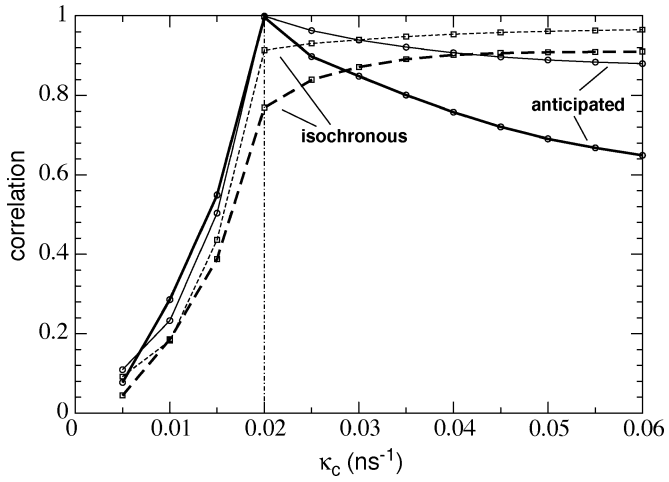

Fig. 4. Correlation for a single-mode (thin lines) and multimode (thick lines) semiconductor lasers. Anticipative (solid lines) and isochronous (dashed lines) synchronization are studied. Note that the maximum in the anticipative synchronization case occurs for the condition $\kappa_c = \kappa_t$ for both single-mode and multimode lasers. At this point, both kind of lasers have the same correlation value for the anticipative synchronization. Spontaneous emission noise is not considered.

indicates the kind of synchronization. For the parameters used in the simulations, a global maximum at $\Delta t = -4$ ns^{-1} corresponds to anticipating synchronization [Fig. 3(a)], while when it is observed at $\Delta t = 0$ it corresponds to isochronous synchronization [Fig. 3(b)]. Also note the existence of relative maxima at different values of Δt from that of the global maximum, although it is that global maximum and its value (close to 0.9) that indicate the kind of synchronization.

Fig. 4 compares the maximum of the correlation function $C(\Delta t)$ corresponding to $\Delta t = 0$ (isochronous synchronization) and $\Delta t = -4$ ns (anticipating synchronization) for a multimode and a single-mode laser with the same parameters. It can be observed that the correlation is in general higher for the single-mode case, in both the anticipative and isochronous situations. In the case of anticipative synchronization, the maximum correlation occurs at $\kappa_t = \kappa_c$, as could be expected and as had been observed in the single-mode case [15]. Furthermore, in that optimal situation the correlation value is identical for the single-mode and the multimode cases (equal to unity, corresponding to a perfect synchronization).

In the generalized (isochronous) case, the correlation increases monotonously with κ_c, both for the single-mode and the multimode case. We now need to examine whether multimode synchronization, despite not being as effective as its single-mode counterpart, is adequate to be used for data transmission. To that end, in Section IV, we will quantify the quality of the encryption compared with the single-mode transmission.

We now analyze how the synchronization quality varies between individual longitudinal modes. Fig. 5 shows the cross-correlation values for the different modes in both the anticipative (upper plot) and isochronous (lower plot) regimes. One can see that although all active modes synchronize, those with higher intensity (namely, the central ones) have a higher correlation as well, whereas the two extreme lateral modes, nearly turned off, have lower correlations. This is due to the fact that, although each mode is injected only by its equivalent (same frequency) peer of the transmitter laser, they are also affected by the behavior of the rest of the longitudinal modes, due to carrier sharing. Since the dominant modes (i.e., those with higher power), are dictating the dynamics of the total power of the laser, the lateral modes are affected not only by their own injection term but also by the dynamics of the higher power modes. A similar behavior is observed in both the anticipated and generalized synchronization (but note the difference in the scales of the y axis between the two plots).

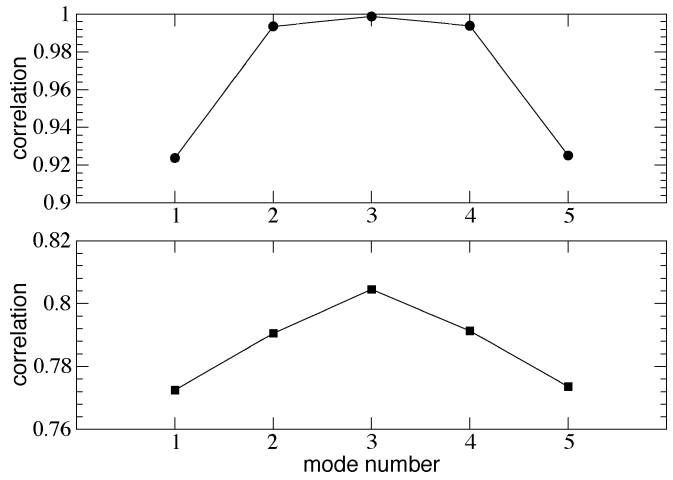

Fig. 5. Cross-correlation coefficient for each individual mode for both the anticipative (upper plot) and isochronous (lower) synchronization, and for $\kappa_c = \kappa_t$ =0.02 ps^{-1}. The mode with higher gain is $m_c = 3$. The modes with higher power also have the higher correlation. Spontaneous emission noise is not considered.

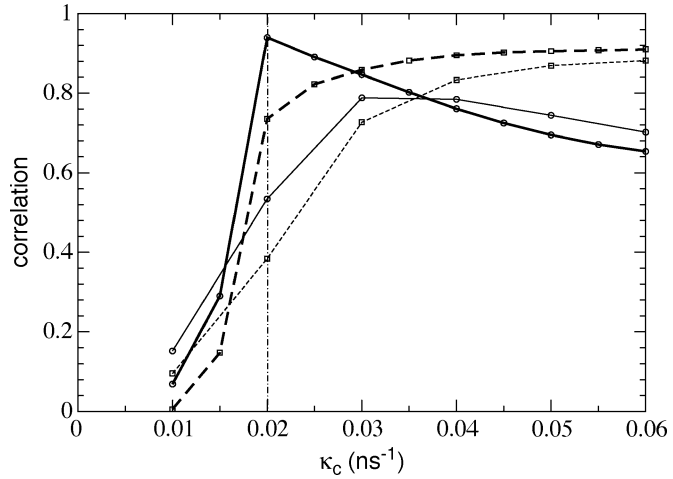

Fig. 6. Comparison between all-to-all injection (thick lines) and selective injection of just one active mode of the transmitter output (thin lines). Anticipative synchronization (solid line) and isochronous synchronization (dashed line) are analyzed. Note that, for the selective injection case, the maximum in the correlation for the anticipative synchronization does no longer occur for $\kappa_c = \kappa_t$, but shifts to higher coupling strengths. In all cases we have included spontaneous emission noise. Spontaneous emission rate is set to $\beta = 5 \times 10^{10}$ ps^{-1}.

It is also interesting to compare the synchronization of two multimode lasers when the injection is global (all modes injected, as considered above), with the situation in which injection is frequency-selective (only one mode from the transmitter is injected into the receiver, i.e., when the filter F in Fig. 1 is present). In what follows, we have only considered selective injection from the central mode of the transmitter laser, which is also the dominant one. Under this configuration, the correlation is never as high as in the case of global injection, due to the fact that less injection means less coupling. In addition to this, the lack of lateral mode injection also reduces the correlation between the lasers. In Fig. 6, we show that the condition for the highest correlation in the anticipated synchronization ($\kappa_c = \kappa_t$ =0.02 ps^{-1}) is not fulfilled anymore. For the frequency-selective case, the maximum in the correlation function shifts to higher couplings and becomes less sharp. The shift in the correlation depends on the ratio between the power of the injected mode and the total power of the transmitter. Concerning the generalized synchronization, no maximum is observed in the correlation, which again increases monotonically with the coupling strength. Note that the peak observed in the correlation of the anticipative synchronization does not arrive to one, as it does in Fig. 4, this slight reduction is due to the inclusion of spontaneous emission noise ($\beta = 5 \times 10^{10}$ ps^{-1}).

Some differences are observed when comparing the results obtained here with those reported in [18] where a different model is considered [19]. In both cases, synchronization of the total output is observed, but in [18] synchronization of the total output does not imply synchronization of the modal outputs, which can be desynchronized. We do not observe this phenomenon: in our simulations, the synchronization of the total output is the consequence of the mode-by-mode synchronization. These results are in accordance with the observations reported in [17], where multimode synchronization is studied with a model of partial differential equations. Another difference with [18] is the absence in our case of "synchronization collapse." Further experimental work should be done in order to clarify the differences between both numerical models.

IV. Message Transmission: Total Output Versus Individual Modes

We now examine systematically the suitability of multimode semiconductor lasers for the transmission of information [17]. We introduce the message into the transmitter by modulating the pumping current of the laser with a periodic bit sequence of 0.1 Gb/s, in what is known as chaos shift keying (CSK) [5]. The chaos filtering properties of the system, originating from the fact that the receiver laser synchronizes only with the chaotic input but not with the message, allows us to recover the message by subtracting the receiver and the transmitter outputs. The laser parameters are those of Table I (with a coupling strength of κ_c =0.02 ps^{-1}), with the exception of the pumping intensity which has been raised to $C = 1.8$ and the inclusion of spontaneous emission noise of intensity $\beta = 5 \times 10^{10}$ ps^{-1} (always considered from now on). The amplitude of the message has been kept to 4.5% of the dc pumping current. With these parameters, the laser operates in the coherence collapse regime (CC) [32], which conceals the emitted message better than the LFF regime. In Fig. 7, we show the total output intensity of the transmitter (a) and the receiver (b). The difference between their outputs is depicted in Fig. 7(c) and its low-pass filtered version in Fig. 7(d). The results show clearly that the bit sequence is satisfactorily recovered.

Since we are working with a multimode semiconductor laser, it is interesting to know how the different longitudinal modes are behaving, and particularly if it is possible to recover the message by using just one or a subset of the longitudinal modes. Fig. 8 shows the message recovered from three longitudinal modes (those which take ~80% of the total power) when all-to-all coupling is considered. We can see how the message is recovered satisfactorily when the total output of both lasers is detected

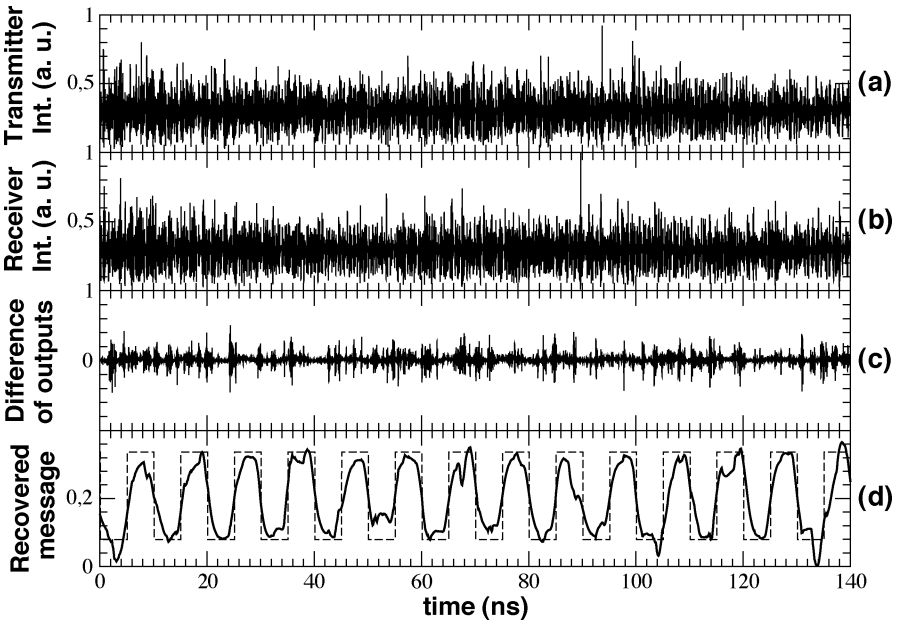

Fig. 7. Output intensities of the (a) transmitter and (b) receiver lasers. (c) The difference between both output signals, which is filtered in (d) and compared with the original message (square wave).

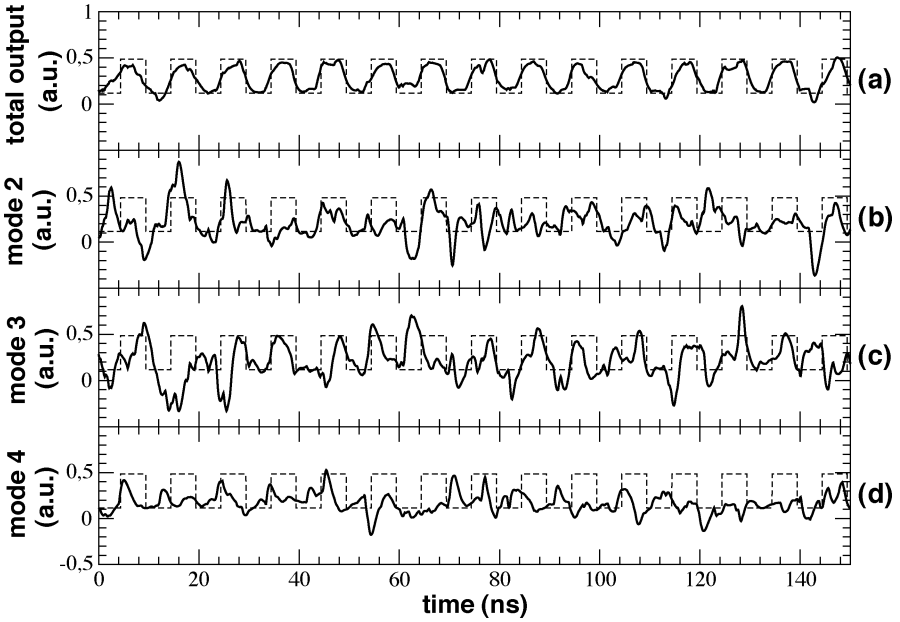

Fig. 8. Recovered message from the signal of (a) all longitudinal modes $N = 5$, (b) mode $m = 2$, (c) mode $m = 3$, and (d) mode $m = 4$. We can observe how the message is not recovered when individual modes are analyzed.

and substracted [Fig. 8(a)], a fact that does not occur when processing single longitudinal modes [Figs. (8b)–(d)]. Our simulations indicate that the power of the message randomly jumps from mode to mode (results now shown), making necessary the detection of the maximum amount of power (and modes) in order to recover the message in an effective way.

V. Message Transmission: Comparing Communication Setups

We now compare different configurations for message transmission with the CSK technique. First, we study message encoding and decoding under conditions of anticipated and generalized synchronization in the open-loop scheme (receiver without feedback). Second, we analyze message transmission in the presence of generalized synchronization in the closed-loop scheme (i.e., receiver laser with feedback, $\kappa_t = \kappa_r$; note that under this condition anticipated synchronization cannot be observed in the closed-loop scheme).

In order to assess the quality of synchronization between the two lasers, we use in what follows, besides the cross-correlation function between their outputs, another indicator of the degree of synchronization, namely the synchronization error $\sigma(t)$

$$\sigma(\Delta t) = \sqrt{\frac{\left\langle \left(P_t(t) - P_r(t+\Delta t)\right)^2 \right\rangle}{\langle P_t(t) \rangle}}. \tag{6}$$

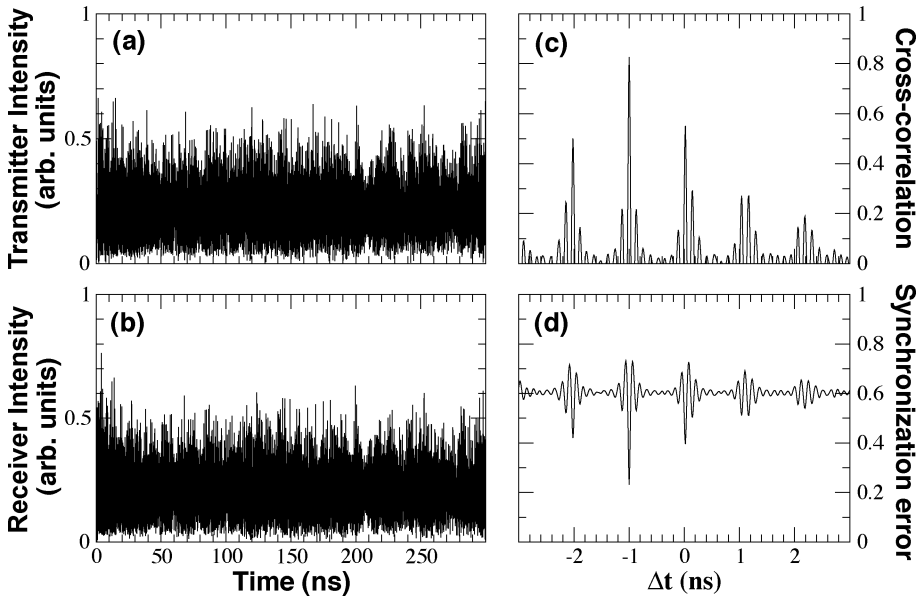

Fig. 9. Output intensities of the (a) transmitter and (b) receiver lasers in the presence of a 100-Mb/s aperiodic bit sequence. The pumping current of both lasers has been set to $C = 1.8$ to force both lasers to emit in the coherence collapse regime. In the right column, we show the cross-correlation coefficient and the synchronization error.

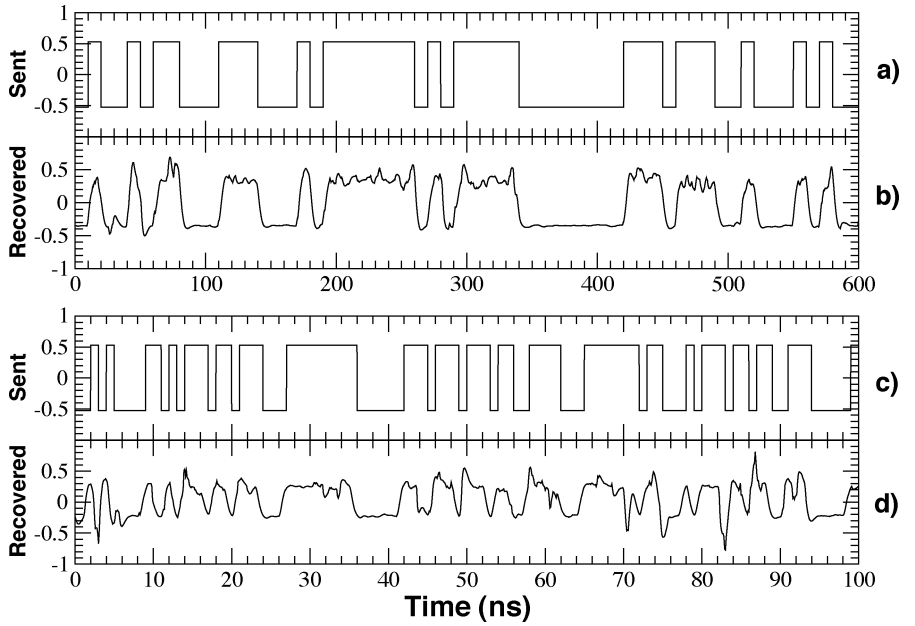

Fig. 10. Recovered message in the open loop scheme for (a), (b) 0.1 Gb/s and (c), (d) 1.0 Gb/s. While for 0.1 Gb/s the message is accurately recovered, it is strongly deteriorated when the transmission speed is increased up to 1.0 Gb/s.

In the case of isochronous synchronization, where $P_r(t) = aP_t(t)$, the output of the receiver can be much higher than that of the transmitter when the coupling strength κ_c exceeds the feedback strength of the transmitter κ_t. This fact would increase the synchronization error. In order to reduce this effect, we have renormalized the output intensity of the receiver via the parameter $a = \langle P_r \rangle / \langle P_t \rangle$. Fig. 9(a) and (b) shows the total intensity of two multimode $(N = 5)$ semiconductor lasers unidirectionally coupled in the open-loop scheme, when an aperiodic 100-Mb/s message has been introduced in the injection current of the transmitter laser with the CSK technique. The amplitude of the message is 4.5% of the dc pumping current, which is low enough to guarantee that the message cannot be recovered by low-pass filtering the transmitter output. The external cavity of the transmitter is set to τ_t =1.0 ns and its feedback strength is κ_t =0.025 ps^{-1}. The coupling strength is set to fulfil the condition for anticipating synchronization (i.e., $\kappa_c = \kappa_t$ =0.025 ps^{-1}). The two lasers become synchronized, as indicated by the cross-correlation function, which shows a maximum $C_{\max} = 0.827$ at $\Delta t = -1$ ns. The location of this maximum indicates that the receiver output is advancing the transmitter a time interval corresponding to τ_t (for the sake of simplicity, the coupling time has been set again to $\tau_c = 0$). The synchronization error also exhibits a minimum

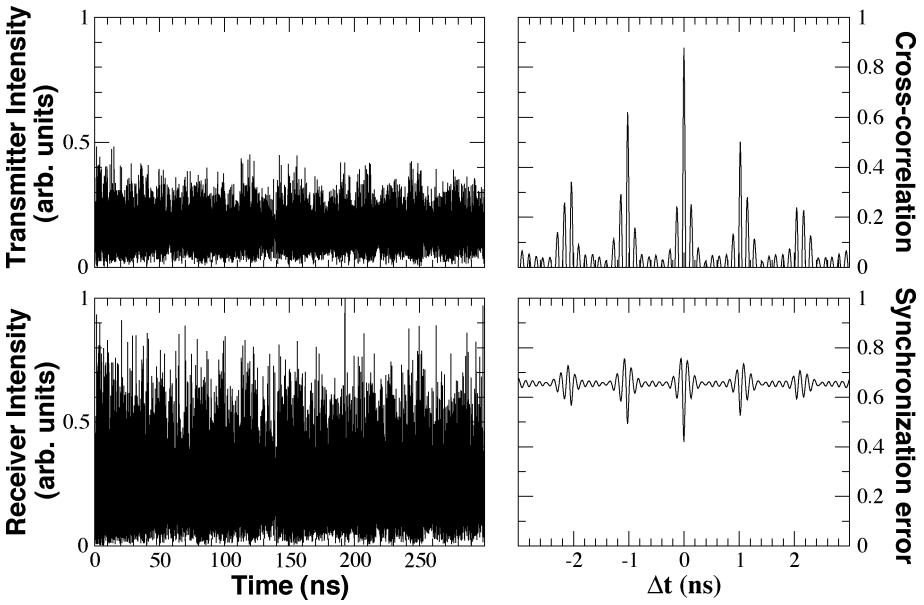

Fig. 11. Output intensities of the (a) transmitter and (b) receiver lasers in the presence of a 0.1-Gb/s nonperiodic bit sequence for the case of generalized synchronization. The right column displays (a) the cross-correlation function and (d) the synchronization error as a function of the time difference between both series.

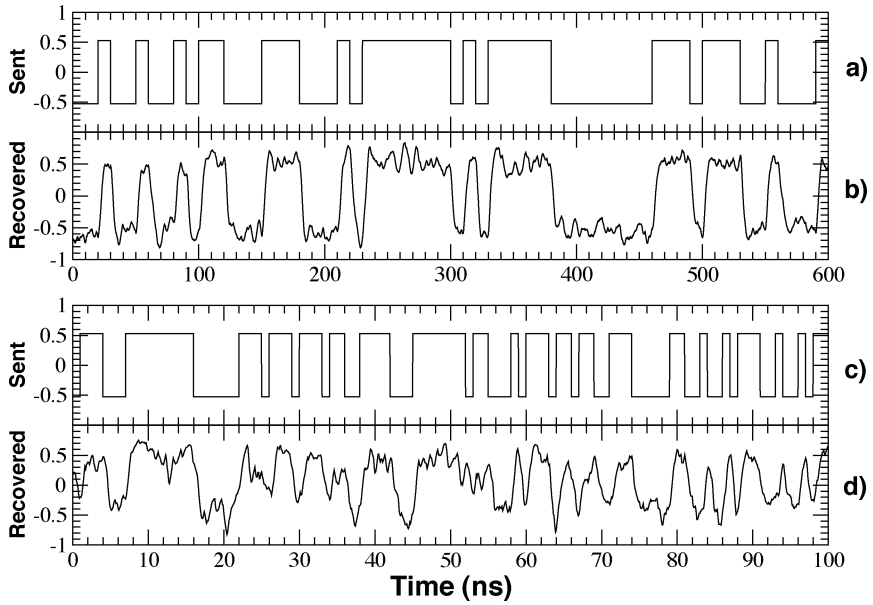

Fig. 12. Recovered message by generalized synchronization in the open-loop scheme for (a), (b) 0.1 Gb/s and (c), (d) 1.0 Gb/s. As in the case of anticipated synchronization, for 0.1 Gb/s the message is accurately recovered, while it is strongly deteriorated when transmission speed is increased to 1.0 Gb/s.

$\sigma_{\min} = 0.231$ at the same value of Δt. The low value of this minimum indicates that this system should be suitable for message transmission.

Subtracting the receiver output to the signal emitted by the transmitter, and filtering the result with a fourth-order Butterworth low-pass filter, should be enough to recover the encrypted message. In Fig. 10 we show the recovered message for 0.1 Gb/s [(a) and (b)] and 1.0 Gb/s [(c) and (d)]. The results indicate that the message is successfully recovered for 0.1 Gb/s, but it is clear that increasing the transmission speed to 1.0 Gb/s strongly degrades the quality of the recovered message up to a point which makes it very difficult to distinguish.

Since generalized synchronization also arises in the open-loop configuration, we now study the efficiency of message recovery based on this type of synchronization. According to Fig. 4, a large coupling coefficient is needed for generalized synchronization to occur. With this aim, we increase the coupling strength up to $\kappa_c = 0.1$ ps^{-1}. Fig. 11 shows the time evolution of the total output intensities of both lasers in this case, together with the cross-correlation function and the synchronization error. We can now see how the receiver laser has considerably increased its output power, due to the high injection coupling. This increase in power (compared with the transmitter) is reflected as an increase of the synchronization error, since this indicator takes into account the absolute difference between the amplitudes of both time series. Note also that, for the case of generalized synchronization, the highest cross-correlation (lowest synchronization error) is observed at $\Delta t = \tau_c$, which

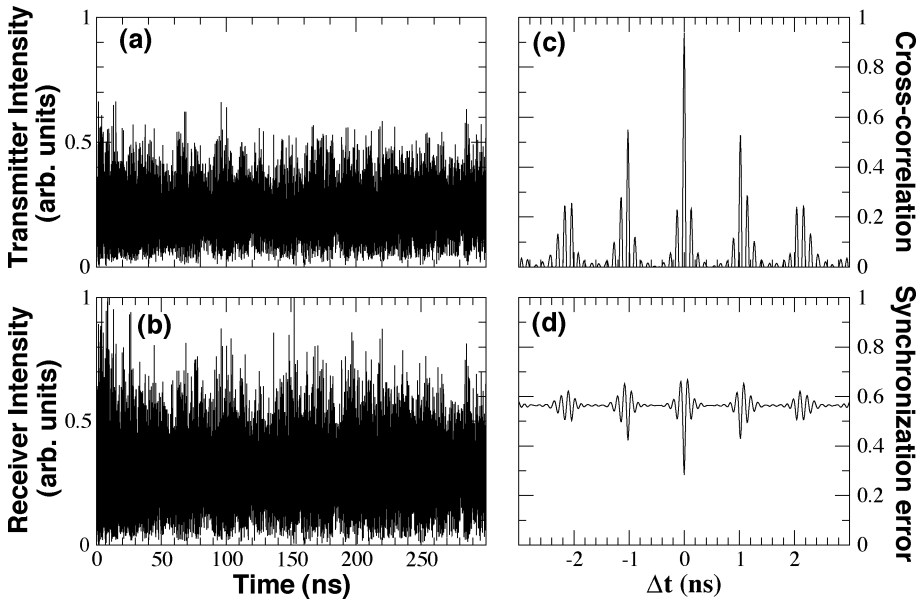

Fig. 13. Output intensities of the (a) transmitter and (b) receiver lasers in the presence of a 0.1-Gb/s nonperiodic bit sequence for the case of closed-loop scheme (and generalized synchronization). The right column displays (a) the cross-correlation function and (d) the synchronization error as a function of the time difference between both series.

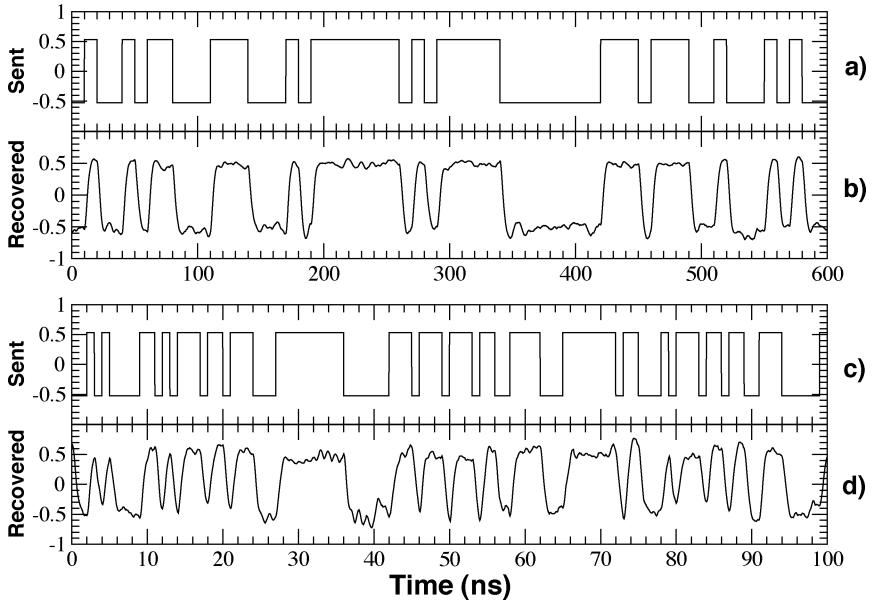

Fig. 14. Recovered message by generalized synchronization in the closed-loop scheme for (a), (b) 0.1 Gb/s and (c), (d) 1.0 Gb/s.

in our case is set to $\tau_c = 0$. Both indicators have values acceptable to, in principle, allow for the efficient recovery of a transmitted message. Finally, we now study the message transmission in the closed-loop scheme, where the receiver laser has external cavity feedback. We consider the same parameters as in the open-loop scheme and generalized synchronization, with the difference that the receiver laser has an external cavity equal to that of the transmitter ($\kappa_r = \kappa_t = 0.025$ ps^{-1} and $\tau_r = \tau_t = 1.0$ ns). Since both lasers are in the same conditions of feedback, and the receiver is in addition injected by the transmitter laser, we will never have identical systems and therefore anticipated synchronization will not be achieved. Nevertheless, it is possible to have generalized synchronization, as can be observed in Fig. 13. This figure shows the total output intensities of the transmitter and receiver lasers and the corresponding cross-correlation and synchronization error. The maximum (minimum) of the cross-correlation (synchronization error) function is obtained for a time delay of $\Delta t = 0$ ns [see Fig. 13(c) and (d)], which is indicative of generalized synchronization.

In Fig. 12, we compare the transmission of a 0.1-Gb/s and a 1.0-Gb/s aperiodic bit sequence. As in the case of anticipated synchronization, the decoding efficiency depends on the transmission speed, with a substantial deterioration of the message for high (1.0 Gb/s) speeds. Nevertheless, message recovery by generalized synchronization is still possible for transmission speeds similar to the case of anticipated synchronization.

When a message is introduced through the transmitter's pumping current, we observe results similar to those obtained in the open-loop configuration. Nevertheless, the closed-loop

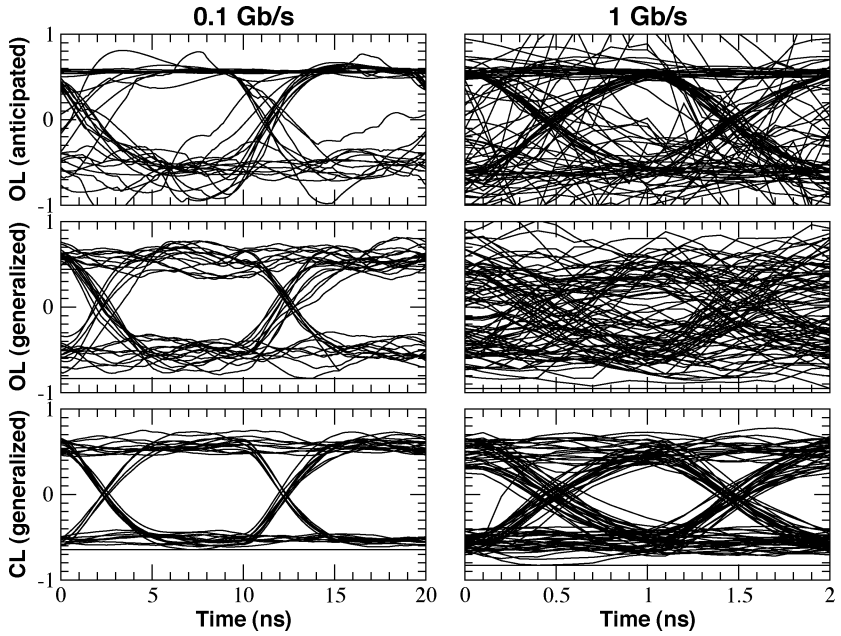

Fig. 15. Eye diagram for the recovered message in the open-loop scheme for the anticipated (first row) and generalized synchronization (second row) and for the closed-loop scheme (third row). Two transmission speeds are shown, 0.1 Gb/s (left column) and 1.0 Gb/s (right column).

configuration seems to be most robust to the increase of the transmission speed, as can be observed in Fig. 14.

In Fig. 15, we summarize and compare the results for the different configurations by plotting the corresponding eye diagrams. One can see how the closed-loop configuration is the most efficient in recovering the message even for high-speed data transmission. In the case of the open-loop scheme, the quality of the recovered message diminishes for high-transmission speeds in both the generalized and anticipated synchronization. For intermediate values of the transmission speed, generalized synchronization works better to recover the encrypted signal (results not shown).

VI. Conclusion

We have studied the anticipative and generalized synchronization of two unidirectionally coupled multimode semiconductor lasers. Both types of synchronization occur mode to mode and, as a consequence, in the total output. We have seen that the degree of synchronization is high enough to allow the use of chaotic multimode lasers in encrypted data transmission. We have also studied the case of selective injection, observing that in that case the anticipative synchronization condition [29] is not fulfilled anymore.

The possibility of using CSK to encode/decode a message has been examined as well. Our results show that the quality of the recovered message is greatly diminished when only a subset of the longitudinal modes is used for decoding. This prevents the use of only part of the modes for message recovery purposes: the sum of all modes (or of a part corresponding to a large portion of the total power) has to be used in order to extract the message. This limitation places a lower bound on the spectral transmission efficiency of the communication channel, since all (or most) modes of the carrier signal must reach the receiver in order for the message to be recovered satisfactorily. Finally, we have compared different configurations to recover a message encrypted by CSK. The results indicate that generalized synchronization in the closed-loop configuration is a more robust setup than the open-loop one, especially when working with high transmission speeds. Additional results (not shown) indicate that anticipating synchronization is strongly deteriorated when moving away from the open-loop toward the close-loop scheme, in agreement with previous simulations in single-mode lasers [15].

In a practical communication system, the signal is usually transmitted to the receiver through an optical fiber. We have not considered in this paper the deteriorating effects of fiber dispersion, losses, and other mechanisms on the quality of synchronization. Examining this issue would be interesting, although we note that previous results in single-mode-laser-based communication systems [3] suggest that synchronization will prevail under those conditions. Further work should also be done in order to clarify whether single-mode or multimode lasers provide a better encryption of the transmitted message, especially from the point of view of the complexity of the chaos generated in both systems.

Acknowledgment

The authors would like to thank C. Mirasso for useful comments.

References

[1] G. D. VanWiggeren and R. Roy, "Communication with chaotic lasers," *Science*, vol. 279, pp. 1198–1200, 1998.

[2] S. Donati and C. R. Mirasso, "Special Issue on Optical Chaos and Applications to Cryptography," *IEEE J. Quantum Electron.*, vol. 38, pp. 1138–1196, Sept. 2002.

[3] C. R. Mirasso, P. Colet, and P. García-Fernández, "Synchronization of chaotic semiconductor lasers: application to encoded communications," *IEEE Photon. Technol. Lett.*, vol. 8, pp. 299–301, Feb. 1996.

[4] V. Annovazzi-Lodi, S. Donati, and A. Scire, "Synchronization of chaotic injected-laser systems and its application to optical cryptography," *IEEE J. Quantum Electron.*, vol. 32, pp. 953–959, June 1996.
[5] A. Sanchez-Diaz, C. R. Mirasso, P. Colet, and P. Garcia-Fernandez, "Encoded Gbit/s digital communications with synchronized chaotic semiconductor lasers," *IEEE J. Quantum Electron.*, vol. 35, pp. 292–297, Mar. 1999.
[6] F. Rogister, A. Locquet, D. Pieroux, M. Sciamanna, O. Deparis, P. Megret, and M. Blondel, "Secure communication scheme using chaotic laser diodes subject to incoherent optical feedback and incoherent optical injection," *Opt. Lett.*, vol. 26, pp. 1486–1488, 2001.
[7] J. P. Goedgebuer, L. Larger, and H. Porte, "Optical cryptosystem based on synchronization of hyperchaos generated by a delayed feedback tunable laser diode," *Phys. Rev. Lett.*, vol. 80, pp. 2249–2252, 1998.
[8] S. Sivaprakasam and K. A. Shore, "Signal masking for chaotic optical communication using external-cavity diode lasers," *Opt. Lett.*, vol. 24, pp. 1200–1202, 1999.
[9] S. Tang and J. M. Liu, "Message encoding-decoding at 2.5 Gbits/s through synchronization of chaotic pulsing semiconductor lasers," *Opt. Lett.*, vol. 26, pp. 1843–1845, 2001.
[10] H. D. I. Abarbanel, M. B. Kennel, L. Illing, S. Tang, H. F. Chen, and J. M. Liu, "Synchronization and communication using semiconductor lasers with optoelectronic feedback," *IEEE J. Quantum Electron.*, vol. 37, pp. 1301–1311, Oct. 2001.
[11] G. D. VanWiggeren and R. Roy, "Optical communication with chaotic waveforms," *Phys. Rev. Lett.*, vol. 81, pp. 3547–3550, 1998.
[12] A. Uchida, S. Yoshimori, M. Shinozuka, T. Ogawa, and F. Kannari, "Chaotic on off keying for secure communications," *Opt. Lett.*, vol. 26, pp. 866–868, 2001.
[13] S. Sivaprakasam and K. A. Shore, "Demonstration of optical synchronization of chaotic external-cavity laser diodes," *Opt. Lett.*, vol. 24, pp. 466–468, 1999.
[14] I. Fischer, Y. Liu, and P. Davis, "Synchronization of chaotic semiconductor laser dynamics on subnanosecond time scales and its potential for chaos communication," *Phys. Rev. A*, vol. 62, no. 4, p. 011801, 2000.
[15] R. Vicente, T. Perez, and C. R. Mirasso, "Open-versus closed-loop performance of synchronized chaotic external-cavity semiconductor lasers," *IEEE J. Quantum Electron.*, vol. 38, pp. 1197–1204, Sept. 2002.
[16] A. Uchida, Y. Liu, I. Fischer, P. Davis, and T. Aida, "Chaotic antiphase dynamics and synchronization in multimode semiconductor lasers," *Phys. Rev. A*, vol. 64, no. 6, p. 023801, 2001.
[17] J. K. White and J. V. Moloney, "Multichannel communication using an infinite dimensional spatiotemporal chaotic system," *Phys. Rev. A*, vol. 59, pp. 2422–2426, 1999.
[18] E. A. Viktorov and P. Mandel, "Synchronization of two unidirectionally coupled multimode semiconductor lasers," *Phys. Rev. A*, vol. 65, no. 4, p. 015801, 2001.
[19] ——, "Low frequency fluctuations in a multimode semiconductor laser with optical feedback," *Phys. Rev. Lett.*, vol. 85, pp. 3157–3160, 2000.
[20] C. L. Tang, H. Statz, and G. deMars, "Spectral output and spiking behavior of solid-state lasers," *J. Appl. Phys.*, vol. 34, pp. 2289–2295, 1963.
[21] F. Rogister, P. Mégret, O. Deparis, and M. Blondel, "Coexistence of in-phase and out-of-phase dynamics in a multimode external-cavity laser diode operating in the low-frequency fluctuations regime," *Phys. Rev. A*, vol. 62, no. 4, p. 061803, 2000.
[22] R. Lang and K. Kobayashi, "External optical feedback effects on semiconductor injection laser properties," *IEEE J. Quantum Electron.*, vol. QE-16, pp. 347–355, Mar. 1980.
[23] T. W. Carr, D. Pieroux, and P. Mandel, "Theory of a multimode semiconductor laser with optical feedback," *Phys. Rev. A*, vol. 63, no. 15, p. 033817, 2001.
[24] M. Yousefi, A. Barsella, D. Lenstra, G. Morthier, R. Baets, S. McMurtry, and J. P. Vilcot, "Rate equations model for semiconductor lasers with multilongitudinal mode competition and gain dynamics," *IEEE J. Quantum Electron.*, vol. 39, pp. 1229–1237, Oct. 2003.
[25] J. M. Buldú, F. Rogister, J. Trull, C. Serrat, M. C. Torrent, J. García-Ojalvo, and C. Mirasso, "Asymmetric and delayed activation of side modes in multimode semiconductor lasers with optical feedback," *J. Opt. B: Quantum Semiclass. Opt.*, vol. 4, pp. 415–420, 2002.
[26] C. Masoller, "Noise-induced resonance in delayed feedback systems," *Phys. Rev. Lett.*, vol. 88, no. 4, p. 034102, 2002.
[27] A. Pikovsky, M. Rosenblum, and J. Kurths, *Synchronization*. Cambridge, U.K.: Cambridge Univ. Press, 2001.
[28] H. U. Voss, "Anticipating chaotic synchronization," *Phys. Rev. E*, vol. 61, pp. 5115–5119, 2000.
[29] C. Masoller, "Anticipation in the synchronization of chaotic semiconductor lasers with optical feedback," *Phys. Rev. Lett.*, vol. 86, pp. 2782–2785, 2000.
[30] C. Risch and C. Voumard, "Self-pulsation in the output intensity and spectrum of GaAs-AlGaAs cw diode lasers coupled to a frequency selective external optical cavity," *J. Appl. Phys.*, vol. 48, pp. 2083–2085, 1977.
[31] V. Ahlers, U. Parlitz, and W. Lauterborn, "Hyperchaotic dynamics and synchronization of external-cavity semiconductor lasers," *Phys. Rev. E*, vol. 58, pp. 7208–7213, 1998.
[32] D. Lenstra, B. Verbeek, and A. J. Boef, "Coherence collapse in single-mode semiconductor laser with external feedback," *IEEE J. Quantum. Electron.*, vol. QE-21, pp. 674–679, June 1985.

Javier M. Buldú was born in Madrid, Spain, in 1974. He received the electrical engineering degree and the Ph.D degree in applied physics from the Universitat Polièctnica de Catalunya (UPC), Terrassa, Spain, in 1998 and 2003, respectively.

After two years working as an electrical engineer, he joined the Department of Physics and Nuclear Engineering, UPC, where his subject of study is the dynamics of semiconductor lasers, on which he has published several articles containing numerical and experimental results. He is currently working on the effects of noise and modulation in semiconductor lasers and the regimes of synchronization of these dynamical systems.

Jordi García-Ojalvo received the Ph.D. degree in physics from the University of Barcelona, Barcelona, Spain, in 1995.

In 1996, he visited the Georgia Institute of Technology, Atlanta, as a Postdoctoral Fellow, and in 1998 he was an Alexander von Humboldt Fellow with the Humboldt Universität zu Berlin, Berlin, Germany. In 2003, he was IGERT Visiting Professor of Nonlinear Systems at Cornell University, Ithaca, NY. Since 1999, he has been an Associate Professor of applied physics with the Universitat Politècnica de Catalunya, Terrassa, Spain. His research interests include spatiotemporal effects in deterministic and stochastic nonlinear systems and dynamics of lasers and nonlinear optical systems.

M. C. Torrent received the B.S., M.S., and Ph.D. degrees in physics from the University of Barcelona, Barcelona, Spain.

In 1991, she joined the Department of Physics and Nuclear Engineering, Politechnical University of Catalonia, Terrassa, Spain, as a Member of the Faculty. Her scientific interests have gradually changed from the theoretical problems in statistical mechanics to applied physics. Her current research is on spatio-temporal dynamics of broad-area lasers and nonlinear dynamics of semiconductor lasers.